tures, but the amplitude was only a few percent of the total concentration of I^-, too small to be observed visually as in the original experiment.

To describe the system more realistically, we must use the five-variable model, Eqs. 1 through 3, because in the experiments the concentrations of the initial reactants at the gel boundaries are a key factor in determining the nature (amplitude and wavelength) of the solution. The relevant case is that in which ClO_2 and I_2 diffuse from one end and MA from the other. We used a finite difference method with 500 mesh points in the 3-mm gel length. With much coarser meshes the inhomogeneity (*23*) (related to the number of peaks) was much larger than with 500 points, but above 400 mesh points the structures were independent of the resolution and were stable in space and time after 7 hours of reaction time. The wavelength, location, and number of peaks are much more sensitive to the diffusion coefficients of I^- and ClO_2^- than to those of ClO_2, I_2, and MA. An example of a calculated stationary structure is shown in Fig. 2.

The experiments of Castets *et al.* (*5*) were conducted on the ClO_2^--I^--MA reaction, whereas the present model treats the simpler ClO_2-I_2-MA system. As Lengyel *et al.* have shown (*6*), ClO_2 and I_2 are formed in the ClO_2^--I^- reaction and then dominate the reaction with MA. However, the generation of ClO_2 and I_2 takes place at some distance into the gel. Unfortunately, there is not yet a detailed mechanism that accounts for the formation of ClO_2 in the ClO_2^--I^- reaction at high ClO_2^- excess. Recent experiments (*24*) show evidence of very similar Turing structures in a ClO_2-I^--MA mixture in the same reactor, lending support to the contention that the model presented here adequately describes the original system.

In retrospect, the discovery of Turing structures in the ClO_2^--I^--MA-starch system appears somewhat fortuitous, in that it is the "inert medium," the gel, by binding key iodine species, that makes it possible to establish the crucial difference in the effective diffusion coefficients of activator and inhibitor. Such circumstances may be rare in inorganic chemical systems. In biological systems, on the other hand, membrane-bound species play key roles, and substrate inhibition, rather than the autocatalysis found in most chemical oscillators, is a common means of dynamical regulation. In such systems, as Turing recognized, diffusion-induced instability is likely to be a major mechanism for pattern formation.

REFERENCES AND NOTES

1. A. M. Turing, *Philos. Trans. R. Soc. London Ser. B* **237**, 37 (1952).
2. J. D. Murray, *J. Theor. Biol.* **98**, 143 (1982).
3. A. R. Peacocke, *The Physical Chemistry of Biological Organization* (Clarendon, Oxford, 1983).
4. J. D. Murray, *Mathematical Biology* (Springer-Verlag, Berlin, 1989).
5. V. Castets, E. Dulos, J. Boissonade, P. De Kepper, *Phys. Rev. Lett.* **64**, 2953 (1990).
6. I. Lengyel, Gy. Rábai, I. R. Epstein, *J. Am. Chem. Soc.* **112**, 4606 (1990).
7. ______, *ibid.*, p. 9104.
8. D. M. Kern and C.-H. Kim, *ibid.* **87**, 5309 (1965).
9. H. Degn and D. E. F. Harrison, *J. Theor. Biol.* **22**, 238 (1969).
10. J. L. Ibañez, V. Fairén, M. G. Velarde, *Phys. Lett. A* **59**, 335 (1976); V. Fairén and M. G. Velarde, *Progr. Theor. Phys.* **61**, 801 (1979).
11. J. P. Kernevez, *Enzyme Mathematics* (North-Holland, Amsterdam, 1980).
12. J. D. Murray, *J. Theor. Biol.* **88**, 161 (1981).
13. G. Nicolis and I. Prigogine, *Self-Organization in Nonequilibrium Systems* (Wiley, New York, 1977); L. A. Segel, *Modeling Dynamic Phenomena in Molecular and Cellular Biology* (Cambridge Univ. Press, New York, 1984); A. B. Rovinsky, *J. Phys. Chem.* **91**, 4606 (1987).
14. L. Edelstein-Keshet, *Mathematical Models in Biology* (Random House, New York, 1988).
15. Gy. Bazsa and M. T. Beck, *Acta Chim. Hung.* **73** 425 (1972).
16. J. Pearson and W. Horsthemke, *J. Chem. Phys.* **90**, 1588 (1989).
17. Nevertheless, there is evidence that similar structures arise in starch-free experiments: Q. Ouyang, K. Lee, H. L. Swinney, unpublished results.
18. S. Hayashi, T. Hirai, S. Shimomichi, N. Hojo, *J. Polym. Sci. Part A* **20**, 839 (1982).
19. A. Cesáro, J. Benegas, D. Ripoli, *J. Phys. Chem.* **90**, 2787 (1986).
20. D. Saunders and R. L. Pecsok, *Anal. Chem.* **40**, 44 (1968).
21. Strictly speaking, the effective reactivity of I^- should also be reduced by this interaction, but we have neglected this much smaller effect in the present treatment.
22. R. Parsons, *Handbook of Electrochemical Constants* (Butterworths, London, 1959).
23. C. Berding, *Bull. Math. Biol.* **49**, 233 (1987).
24. P. De Kepper and I. Nagypál, unpublished results.
25. I. Ruff, V. J. Friedrich, K. Csillag, *J. Phys. Chem.* **76**, 162 (1972).

26. We thank P. De Kepper and J. Boissonade for discussions of Turing structures and for encouraging us to probe more deeply into the mechanism of this system. This work was supported by grants from the National Science Foundation (CHE-8800169) and by a U.S.–Hungarian cooperative grant from the National Science Foundation and the Hungarian Academy of Sciences.

31 July 1990; accepted 8 November 1990

Potassium in Clinopyroxene Inclusions from Diamonds

GEORGE E. HARLOW AND DAVID R. VEBLEN

Analytical transmission electron microscopy, electron microprobe analyses, and single-crystal x-ray diffraction data support the conclusion that high potassium contents, up to 1.5 weight percent K_2O, of some diopside and omphacite inclusions from diamonds represent valid clinopyroxene compositions with K in solid solution. This conclusion contradicts the traditional view of pyroxene crystal chemistry, which holds that K is too large to be incorporated in the pyroxene structure. These diopside and omphacite inclusions have a high degree of crystal perfection and anomalously large unit-cell volumes, and a defect-free structure is observed in K-bearing regions when imaged by transmission electron microscopy. These observations imply that clinopyroxene can be a significant host for K in the mantle and that some clinopyroxene inclusions and their diamond hosts may have grown in a highly K-enriched environment.

THE QUESTION OF WHERE SUBSTANTIAL K resides in the mantle is fundamental for understanding the source for K in basalts that originate from partial melting of the mantle, the distribution of K in the mantle, the role of K in mantle metasomatism and diamond formation, and the mantle's heat budget (because of radioactive decay of ^{40}K). Garnet peridotites are thought to have compositions typical of the upper mantle, and among the nominally anhydrous solid phases in these rocks, diopsidic clinopyroxene (approximately $CaMgSi_2O_6$) has the highest K level, is stable over a large range of pressures, and is reasonably abundant. However, measured levels of K in clinopyroxene (cpx) from garnet peridotite xenoliths in kimberlites and other extrusive rocks are too small to account for the K levels in basalts produced by partial melting (*1*). Eclogites are closer to basalts in composition, and their K-bearing phases may include sanidine as well as omphacite (a cpx with a nominal composition of $Na_{0.5}Ca_{0.5}Al_{0.5}Mg_{0.5}Si_2O_6$). Although eclogites may be important reservoirs for K, they are not considered to be the source of most mantle-derived basalts. Moreover, the relatively high K contents of omphacite from Group I eclogite xenoliths (0.10 to 0.33% K_2O by weight) have not been demonstrated to be in the cpx crystal structure (*2*). In order to evaluate accurately the potential for cpx as a K reservoir in the mantle and as a possible source for K in the genesis of mantle-derived igneous rocks, the crystal chemistry of K in pyroxene must be understood better and reconciled with measurements on xenolith suites.

G. E. Harlow, Department of Mineral Sciences, American Museum of Natural History, New York, NY 10024.
D. R. Veblen, Department of Earth and Planetary Sciences, The Johns Hopkins University, Baltimore, MD 21218.

Conventional wisdom holds that K is too large to fit or partition into M2, the largest crystallographic site in the clinopyroxene structure (*3–6*). For example, Papike (*6*, p. 505) stated that "the only major element that cannot be accommodated in the pyroxene structure is K. . . ." In this view, the nominal ionic radius $r = 1.51$ Å for K^+ in eightfold coordination is simply too great for the M2 coordination sphere, which accepts alkali and alkaline earths only as large as Na^+ and Ca^{2+}, which have radii of ~1.2 Å. Most early observations of high K contents (≥0.5% K_2O by weight) by bulk or electron microprobe analysis of pyroxenes have been discredited as artifacts produced by contamination from other phases in cracks, inclusions, or fine-scale intergrowths (*7–9*). The notion that K cannot enter the pyroxene structure may have been biased by a focus on relatively low-pressure crustal samples and a continued disbelief in the structural integrity of pyroxenes from the mantle reported with high K contents, even though the latter have been used successfully to differentiate between Group I and Group II mantle eclogites and to establish the comparability of Group I and diamondiferous eclogites (*2*).

Table 2. Lattice parameters determined by least-squares refinement of single-crystal x-ray diffractometer measurements.

Lattice parameters	K18a	K14a1	OR20	MPD18	MPD42
a (Å)	9.7476(4)	9.723(4)	9.602(3)	9.659(1)	9.640(1)
b	8.9478(4)	8.921(4)	8.785(3)	8.847(1)	8.836(1)
c	5.2622(2)	5.257(2)	5.261(2)	5.266(1)	5.2556(3)
β (degrees)	106.056(2)	106.26(3)	106.84(2)	106.57(1)	106.59(1)
V (Å^3)	441.06(3)	437.7(3)	424.7(2)	429.00(7)	431.4(1)

(Column group heading: Clinopyroxene sample)

Table 1. Representative electron microprobe analyses of K-rich clinopyroxene inclusions in diamonds and coexisting phases. Samples: K18a, Cr-rich diopside, Koffiefontein Mine, South Africa (1 for Capetown probe and 2 for AMNH probe analyses); K14a1, diopside, Koffiefontein Mine (1 for Capetown probe analysis, 2 for Johns Hopkins AEM analysis of a region shown by HRTEM to be nondefective pyroxene); OR20, omphacite, Orapa Mine, Botswana; MPD42, omphacite, locality unknown; and MPD18, omphacite, locality unknown. K18a, K14a1, and OR20 are from J. Gurney (*13, 15*), and MPD42 and MPD18 are from M. Prinz (*12*). Fe_2O_3 and Fe^{3+} contents were determined by cation sum and charge balancing. Coexisting phases are gar, garnet; mag, magnetite; olv, olivine; opx, orthopyroxene; phl, phlogopite; and rut, rutile.

Component	K18a(1)	K18a(2)	K14a1(1)	K14a1(2)	OR20	MPD42	MPD18
			Oxides (weight percent)				
SiO_2	54.3	55.0	54.7	55.8	54.9	56.0	54.7
TiO_2	0.01	0.01	0.03	0.02	0.63	0.33	0.25
Al_2O_3	0.68	0.60	1.55	1.39	11.5	8.60	7.60
Cr_2O_3	2.44	2.57	0.89	1.07	0.07	0.19	0.18
Fe_2O_3	0.17	1.07	0.0	0.0	0.0	0.0	0.0
FeO	1.76	1.11	2.40	2.50	4.85	4.70	6.40
MnO	0.08		0.09	0.05	0.06	0.07	0.11
MgO	17.5	17.1	18.5	18.4	8.56	11.2	10.4
CaO	20.3	20.5	20.1	19.3	12.7	15.1	15.6
Na_2O	0.33	0.23	0.45	0.54	5.79	4.10	3.80
K_2O	1.57	1.71	0.79	0.88	0.38	0.62	0.87
Total	99.1	99.9	99.5	99.9	99.4	100.9	99.9
			Cations for six oxygens				
Si	1.99	2.00	1.99	2.01	1.97	1.99	1.99
Al^{IV}	0.008	0.00	0.015	0.00	0.033	0.014	0.015
Ti	0.000	0.000	0.001	0.001	0.017	0.009	0.007
Al^{VI}	0.021	0.026	0.051	0.059	0.45	0.35	0.31
Cr	0.071	0.074	0.026	0.030	0.002	0.005	0.005
Fe^{3+}	0.005	0.029	0.000	0.000	0.000	0.000	0.000
Fe^{2+}	0.054	0.034	0.073	0.075	0.15	0.14	0.19
Mn	0.002		0.003	0.002	0.002	0.002	0.003
Mg	0.96	0.93	1.00	0.99	0.46	0.59	0.56
Ca	0.80	0.80	0.78	0.74	0.49	0.57	0.61
Na	0.023	0.016	0.032	0.038	0.40	0.28	0.27
K	0.073	0.079	0.037	0.040	0.017	0.028	0.040
Total	4.00	3.98	4.00	3.98	3.98	3.98	4.00
Coexisting phases	opx, olv		none		none	gar, mag	phl, rut

Clinopyroxene inclusions in diamonds are ideal samples for studying K in mantle pyroxene because these inclusions have not been affected by alteration and obviously are associated with the formation of diamond at high pressures. A few crystals with remarkably high K contents (>0.2% K_2O) (*10–12*) have been reported in earlier studies of such inclusions. Most of these high-K inclusions are omphacites representative of the mantle eclogite suite (*12, 13*), and a few are diopsides or chromium diopsides representative of the ultramafic suite (garnet lherzolites) (*14, 15*).

In this report we present new crystal chemical data from cpx inclusions in five diamonds and show that cpx can contain structural K in amounts up to 1.5% K_2O (0.07 K atoms per M2 site). Sources, coexisting phases (*16*), and electron microprobe analyses for the samples are listed in Table 1. Each sample is a single crystal that ranges from 50 to 140 μm in maximum dimension to 20 μm in the smallest. The crystals are either rounded and irregular or somewhat xenohedral, mimicking an octahedral form (*10, 12*). The crystals are all completely transparent and gemmy, without visible inclusions, except for K18a, which contains a lath of orthopyroxene.

The electron microprobe analyses (Table 1) indicate that the crystals are homogeneous at the resolution of the technique and have good pyroxene stoichiometry. Maximum vacancies are 0.022 per four total cations or per M2 site; thus, vacancies do not play a major role in these mantle pyroxenes, unlike those studied by McCormick *et al.* (*17*). There are sufficient trivalent cations (less Tschermak's component) to charge balance the measured monovalent cations in every case, if K is assumed to be present in the pyroxene structure.

Each crystal was examined with single-crystal x-ray diffraction to evaluate both crystallinity and lattice dimensions. Long-exposure precession photographs (>100 hours, Mo Kα radiation, Zr filter) show only sharp Bragg diffractions consistent with cpx having space group *C2/c*. There are no extra spots from another phase (except orthopyroxene in K18a) and no diffuse streaks or anisotropic spots that might suggest the presence of extended defects or intergrowths that could account for the observed K. Unit-cell parameters (Table 2) were determined from least-squares refinement of approximately 50 reflections (averaged positive and negative 2θ, where

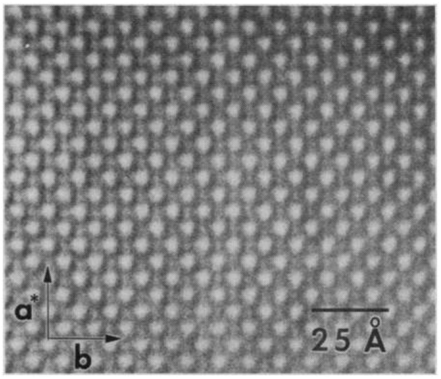

Fig. 1. A *c*-axis HRTEM image of K-rich diopside K14a1 displaying the I-beam structure characteristic of ordered, nondefective pyroxene. An AEM analysis obtained from within the area of this image is given as K14a1 (*2*) in Table 1 and is comparable with the electron microprobe analysis K14a1 (*1*).

$35° < 2\theta < 55°$) measured with a single-crystal diffractometer (Mo Kα radiation, method standardized on quartz).

If the large K cation is incorporated in the pyroxene structure, it should demonstrably affect the lattice parameters. Because there is no general empirical or theoretical model for estimating cpx unit-cell parameters from the chemical composition, we have used a linear model for the relation between the unit-cell cation numbers and cell volume, *V*, based on both literature data and data from this study (see Table 3). In order to reduce the variance of the chemical composition, minor elements were lumped with similar major cations (Cr and V with Fe^{3+}; Mn and Ni with Fe^{2+}). Silicon was considered indirectly by evaluating Al^{IV}. Two models were considered: Model 1 includes K as a cation variable, whereas Model 2 is without K. Table 3 shows that the deviations for *V* are essentially random with respect to K content for Model 1, whereas, excluding DHZ4B, they show a definite positive trend with K content in Model 2 and exceed the standard error of estimate significantly for the most K-rich cpx, K18a. The unit-cell volumes of the five cpx from diamonds are thus poorly predicted when K is not considered to be in solid solution. This analysis supports the notion that K is incorporated structurally in a manner consistent with its large ionic radius.

Recent studies have shown that analytical and high-resolution transmission electron microscopy (AEM and HRTEM) are powerful tools for determining whether an element is in solid solution. For example, these methods were used to show that Cu in high-Cu biotites is present as submicroscopic inclusions of native Cu, not in solid solution as a true biotite component (*18*). Therefore, for additional evidence that K is in solid solution in the cpx inclusions, we examined diopside K14a1 with AEM and HRTEM using a Philips 420ST instrument (*19*). Part of the crystal was crushed and deposited on a holey carbon grid. For all of the approximately dozen fragments, observations were made in both bright-field and dark-field modes, x-ray emission spectra were collected to verify composition, and HRTEM images down major zones were examined. All of the fragments consisted of homogeneous, structurally intact cpx and possessed compositions consistent with the electron microprobe analyses, that is, the analyses indicated the presence of homogeneously distributed K (Table 1). No stacking faults or chain width errors were found (Fig. 1); two dislocations were the only defects observed among all the fragments. The only conclusion is that K resides in the structure of this cpx, not in extended defects or other included phases.

Thus, substantial amounts of K can be incorporated in cpx that grows at the high-pressure conditions required for diamond formation in the mantle (>5 GPa). Detailed discussion of the crystal chemistry of these high-K pyroxenes must await complete crystal structure refinements. However, it is clear from the chemical analyses, unit-cell parameters, and TEM observations that the K must be entering one of the cpx crystallographic cation sites, and the M2 site is the only likely candidate.

On the basis of the crystals we examined, diopsidic cpx appears to be a better host for K than omphacite or jadeite. With a nominal unit-cell *V* of ~439 $Å^3$, a diopside with limited substitution of trivalent cations for charge balancing should accept more K than omphacite ($V \approx 425$ $Å^3$) or especially jadeite ($NaAlSi_2O_6$; $V \approx 419$ $Å^3$). The more expanded structure of diopside is attributed primarily to the presence of Mg or Fe^{2+} in the M1 site, versus substantial Al^{3+} in omphacite and jadeite. Charge balancing of K by substitution of Cr^{3+} or Fe^{3+} ($r = 0.615$ or 0.645 Å), which are larger than Al^{3+} ($r = 0.535$ Å), may further assist in expanding the M2 site for occupancy by K^+. Thus, K may be more soluble in diopside than in omphacite under the same conditions.

A practical question is whether K content could be used as a geobarometer. In exper-

Table 3. Results of regressions for linear models relating clinopyroxene cell volume to cation values Al^{IV}, Al^{VI}, Ti, Fe^{3+}, Mg, Fe^{2+}, Ca, Na, and either including K (Model 1) or excluding K (Model 2). Data for both models are from 20 clinopyroxenes analyses in Deer *et al.* (*4*) (numbers: 6A, 7A, p. 431; 4B, 6B, 7B, 8B, 10B, 12B, pp. 433–435), Cameron and Papike (*3*) (all CP numbers), and Nybö omphacite (*27*); plus, only for Model 1, six clinopyroxenes from this study. V_{obs} and V_{calc} are observed and calculated cell volumes. The calculated values for $K18a_{(1)}$ and $K18a_{(2)}$ represent the two microprobe analyses from Table 1. Model 2 shows differences either without K (ignored) or for K summed with Na. For Model 1 the SE is 0.79; regression coefficients (and coefficient errors) are Al^{IV}, −24.60 (5.0); Al^{VI}, 37.78 (12.); Ti, 73.31 (15.); Fe^{3+}, 64.27 (12.); Mg, 30.13 (8.5); Fe^{2+}, 43.61 (8.5); Ca, 40.71 (8.0); Na, −1.91 (6.5); K, 69.79 (11.); intercept, 366.46 ($Å^3$).

Sample	K cations	V_{obs} ($Å^3$)	$V_{obs} - V_{calc}$		
			Model 1	Model 2	
			w K	w/o K	(K as Na)
DHZ6A	0.002	426.73	0.57	0.70	0.70
DHZ7A	0.000	427.02	−0.93	−0.94	−0.94
DHZ4B	0.000	421.60	−1.83	−1.87	−1.87
DHZ6B	0.001	424.66	1.04	1.08	1.08
DHZ7B	0.000	424.60	0.28	−0.31	−0.31
DHZ10B	0.002	428.91	0.03	0.04	0.04
CP72	0.002	428.85	0.55	0.57	0.57
CP73	0.000	423.90	−0.93	−0.95	−0.95
CP74	0.000	420.20	−0.11	−0.16	−0.16
CP29	0.000	429.90	1.00	0.99	0.99
CP71	0.000	423.50	0.40	−0.42	−0.42
DHZ12B	0.000	426.81	0.56	0.53	0.53
Nybö	0.000	414.50	0.24	0.18	0.18
CP24C	0.000	431.60	−0.83	−0.80	−0.80
CP24	0.000	431.90	0.54	0.62	0.62
CP6	0.002	401.20	0.10	0.19	0.19
CP8	0.000	429.10	0.14	0.12	0.12
CP15	0.000	421.35	0.15	0.15	0.15
CP2	0.000	438.60	0.49	0.45	0.45
CP4	0.000	450.60	−0.17	−0.17	−0.17
OR20	0.017	424.73	0.21	1.35	1.39
MPD18	0.028	429.00	−0.02	1.91	1.97
K14a1	0.037	437.73	0.18	2.79	2.88
MPD42	0.040	431.35	−0.09	2.68	2.77
$K18a_{(1)}$	0.073	441.06	0.31	5.41	5.58
$K18a_{(2)}$	0.079	441.06	−0.40	5.10	5.28

iments with a garnet peridotite composition containing anhydrous phlogopite at 3.8 to 10 GPa and 1350° to 1400°C, the K content of diopside increased with increasing pressure up to 0.26% K_2O by weight at 10 GPa (*20*). Extrapolation to K contents as high as that in diopside K18a yields a high pressure, >20 GPa, which is probably beyond the stability field of diopside, but there is great uncertainty in the estimated temperatures for this inclusion and Koffiefontein xenoliths. Garnet-cpx assemblages give temperatures from 1000° to 1550°C (*21*), whereas the two K18 chromium diopside inclusions are in disequilibrium, yielding olivine-cpx temperatures of 1033° and 1233°C (*15*). Two-pyroxene geothermometry gives temperatures from 1000° to 1350°C at ~5 GPa (uncorrected for K content, of course) (*22–25*). Certainly, further experiments on the solubility of K in cpx are required to interpret the pressure conditions under which substantial K can enter pyroxenes. In any case, the K content of cpx cannot be used as a geobarometer in the absence of other K-bearing phases. This limitation is a particular problem with diamond inclusions. Alone, the implication of the presence of high K contents in cpx is that formation under high pressure is required, but K contents of cpx will vary with the total amount of K in the rock and the other phases present.

The high levels of K in these clinopyroxenes suggest that the host diamonds formed in unusually K-rich environments. Navon *et al.* (*26*) have described inclusions from morphologically cubic diamonds containing high levels of K, CO_2, and H_2O and suggested that potassic melts or metasomatic fluids in the mantle were responsible for the enrichments. As already noted, K in omphacite has been used as a marker for Group I eclogites (*2*), which are the eclogites that contain diamond. This relation reinforces the connection between these K-rich melts or fluids, diamonds, and K-rich cpx.

REFERENCES AND NOTES

1. A. J. Erlank and I. Kushiro, *Carnegie Inst. Washington Yearb.* **68**, 233 (1970).
2. T. E. McCandless and J. J. Gurney, in *Kimberlites and Related Rocks*, J. Ross *et al.*, Eds. (*Geol. Soc. Aust. Spec. Publ. 14*, Blackwell, Victoria, 1989), vol. 2, pp. 827–832; I. D. MacGregor and W. I. Manton, *J. Geophys. Res.* **91**, 14063 (1988); D. N. Robinson, J. J. Gurney, S. R. Shee, in *Kimberlites II: The Mantle and Crust-Mantle Relationships*, J. Kornprobst, Ed. (*Develop. Petrol.* **11B**, Elsevier, Amsterdam, 1984), pp. 11–24.
3. M. E. Cameron and J. J. Papike in *Pyroxenes*, C. T. Prewitt, Ed. (*Rev. Mineral.* 7, Mineralogical Society of America, Washington, DC, 1980), pp. 5–92.
4. W. A. Deer, R. A. Howie, J. Zussman, *Single-Chain Silicates*, vol. 2A of *Rock-forming Minerals* (Wiley, New York, NY, 1978).
5. N. Morimoto *et al.*, *Am. Mineral.* 73, 1123 (1988).
6. J. J. Papike, in *Pyroxenes*, C. T. Prewitt, Ed. (*Rev. Mineral.* 7, Mineralogical Society of America, Washington, DC, 1980), pp. 495–525.
7. A. J. Erlank, *Carnegie Inst. Washington Yearb.* **68**, 433 (1970).
8. M. Mellini and A. Cundari, *Mineral. Mag.* **53**, 311 (1989).
9. D. R. Veblen and P. R. Buseck, *Am. Mineral.* **66**, 1107 (1981).
10. H. O. A. Meyer, in *Mantle Xenoliths*, P. H. Nixon, Ed. (Wiley, New York, NY, 1987), pp. 501–524.
11. J. J. Gurney, J. W. Harris, R. S. Rickard, in *Kimberlites, Diatremes, and Diamonds: Their Geology, Petrology, and Geochemistry*, F. R. Boyd and H. O. A. Meyer, Eds. (American Geophysical Union, Washington, DC, 1979), pp. 1–15.
12. M. Prinz *et al.*, *Phys. Chem. Earth* **9**, 797 (1975).
13. J. J. Gurney, J. W. Harris, R. S. Rickard, in *Kimberlites II: The Mantle and Crust-Mantle Relationships*, J. Kornprobst, Ed. (*Develop. Petrol.* **11B**, Elsevier, Amsterdam, 1984), pp. 3–9.
14. H.-M. Tsai, H. O. A. Meyer, J. Moreau, H. J. Milledge, in *Kimberlites, Diatremes, and Diamonds: Their Geology, Petrology, and Geochemistry*, F. R. Boyd and H. O. A. Meyer, Eds. (American Geophysical Union, Washington, DC, 1979), pp. 16–26.
15. R. S. Rickard, J. W. Harris, J. J. Gurney, P. Cardoso, in *Kimberlites and Related Rocks*, J. Ross *et al.*, Eds. (*Geol. Soc. Aust. Spec. Publ.* **14**, Blackwell, Victoria, 1989), vol. 2, pp. 1054–1062.
16. It is not totally clear, particularly with respect to the inclusions described by Prinz *et al.* (*12*), whether the phases are truly coexisting—in mutual contact—or only found in the same diamond.
17. T. C. McCormick, R. M. Hazen, R. J. Angel, *Am. Mineral.* 74, 1287 (1989).
18. E. S. Ilton and D. R. Veblen, *Nature* **334**, 516 (1988).
19. Because a sample must be partially crushed or otherwise diminished in size in order to carry out TEM study, K14a1 was selected instead of K18a, which has greater K content, so that K18a could be left intact for future study.
20. N. Shimizu, *Earth Planet. Sci. Lett.* **11**, 374 (1971).
21. W. L. Griffin *et al.*, in *Extended Abstracts, Workshop on Diamonds*, F. R. Boyd *et al.*, Eds. (Geophysical Laboratory, Carnegie Institution of Washington, Washington, DC, 1989), pp. 23–25.
22. A. A. Finnerty and F. R. Boyd, in *Mantle Xenoliths*, P. H. Nixon, Ed. (Wiley, New York, NY, 1987), pp. 381–402.
23. D. H. Lindsley and S. A. Dixon, *Am. J. Sci.* **276**, 1285 (1976).
24. G. Brey, T. Köhler, K. Nickel, in *Extended Abstracts, Workshop on Diamonds*, F. R. Boyd *et al.*, Eds. (Geophysical Laboratory, Carnegie Institution of Washington, Washington, DC, 1989), pp. 8–10.
25. R. L. Hervig and J. V. Smith, *J. Geol.* **88**, 337 (1980).
26. O. Navon, I. D. Hutcheon, G. R. Rossman, G. J. Wasserburg, *Nature* **335**, 784 (1987).
27. D. C. Smith, A. Mottana, G. Rossi, *Lithos* **13**, 227 (1980).

28. We thank two anonymous reviewers for constructive comments. The specimens used in this study (Table 1) were supplied by J. Gurney and M. Prinz. This work was funded by the American Museum of Natural History and the National Science Foundation.

14 September 1990; accepted 11 December 1990

The Search for Evidence of Large Prehistoric Earthquakes Along the Atlantic Seaboard

DAVID AMICK AND ROBERT GELINAS

The spacial distribution of seismically induced liquefaction features discovered along the Atlantic seaboard suggests that during the last 2000 to 5000 years, large earthquakes (body wave magnitude, $m_b \geq 5.8 \pm 0.4$) in this region may have been restricted exclusively to South Carolina. Paleoliquefaction evidence for six large prehistoric earthquakes was discovered there. At least five of these past events originated in the Charleston, South Carolina, area, the locale of a magnitude 7+ event in 1886. During the past two millennia, large events may have occurred about every 500 to 600 years.

THE LARGEST HISTORICAL EARTHQUAKE in the eastern United States occurred near Charleston, South Carolina, in August 1886. The proximity of this magnitude 7+ event to populated areas made it the most destructive U.S. earthquake of the 19th century (*1*). Today a similar earthquake could result in several thousand deaths and property damage in excess of $400 million (*2*). Clearly, the potential for another large earthquake near Charleston or elsewhere along the Atlantic seaboard must be assessed. This task is especially difficult because Charleston lies far from an active plate boundary in a region where no comparable historical earthquakes have occurred and where there is no clear paleoseismic evidence of surface faulting associated with large prehistoric events (*3*).

Although the bedrock faulting responsible for the Charleston earthquakes has not reached the ground surface, strong ground shaking associated with the 1886 and earlier events resulted in the formation of numerous seismically induced liquefaction (*4–6*) features in surficial sediments (Fig. 1). The results of past studies suggest that the return period between large ($m_b \geq 5.8 \pm 0.4$) earthquakes is about 1500 years (*7–9*). In this report, we synthesize published and newly acquired paleoliquefaction data and show that the frequency of large (*10*) earthquakes occurring near Charleston is greater than previously established. We also report

---

Ebasco Services Incorporated, 2211 West Meadowview Road, Greensboro, NC 27407.